1-1-2002

X-ray photoelectron spectroscopic investigation of surface chemistry of ternary As-S-Se chalcogenide glasses

Wenyan Li
University of Central Florida

Sudipta Seal
University of Central Florida

Cedric Lopez
University of Central Florida

Kathleen A. Richardson
University of Central Florida

Recommended Citation

Li, Wenyan; Seal, Sudipta; Lopez, Cedric; and Richardson, Kathleen A., "X-ray photoelectron spectroscopic investigation of surface chemistry of ternary As-S-Se chalcogenide glasses" (2002). *Faculty Bibliography 2000s*. 3316.
https://stars.library.ucf.edu/facultybib2000/3316

X-ray photoelectron spectroscopic investigation of surface chemistry of ternary As–S–Se chalcogenide glasses

Wenyan Li, Sudipta Seal, Cedric Lopez, and Kathleen A. Richardson

View Online   Export Citation

ARTICLES YOU MAY BE INTERESTED IN

X-ray photoelectron spectroscopic investigation of surface chemistry of ternary As–S–Se chalcogenide glasses

Wenyan Li and Sudipta Seal[a)]
Advanced Materials Processing and Analysis Center and Mechanical, Materials and Aerospace Engineering, University of Central Florida, Orlando, Florida 32816

Cedric Lopez
School of Optics and The Center for Research and Education in Optics and Lasers, University of Central Florida, Orlando, Florida 32816

Kathleen A. Richardson
Advanced Materials Processing and Analysis Center and Mechanical, Materials and Aerospace Engineering, University of Central Florida, Orlando, Florida 32816 and School of Optics and The Center for Research and Education in Optics and Lasers, University of Central Florida, Orlando, Florida 32816

Chalcogenide glasses belong to an important class of materials, due to their good infrared transmission, and low-phonon energy as compared to other oxide glasses. Structural and chemical variations imposed by glass processing conditions, e.g., film deposition, can lead to changes in the linear and nonlinear optical properties. X-ray photoelectron spectroscopy (XPS) has been employed to study As–S–Se glasses of differing chemical compositions, in the film and the bulk form, to understand any variations in chemical bond configuration and their electronic structure. The molecular environments of As and Se for As–S–Se samples with varying S/Se ratio (fixed As content) and As content (fixed S/Se ratio) are studied by monitoring the XPS chemical shifts. The surface chemistry of the bulk and thin-film chalcogenide glasses are also compared to determine the effect of glass processing conditions for better chalcogenides for potential waveguide applications. © *2002 American Institute of Physics.* [DOI: 10.1063/1.1518134]

I. INTRODUCTION

Chalcogenide glasses have attracted considerable interest due to their infrared transparency, low-phonon energies, and high-nonlinear optical parameters.[1–5] They are promising materials for grating and switching devices, and optical memories.[6–9] Recently, these glasses have been used as core materials for high-efficiency fiber amplifiers due to their high-refractive indices and very low-phonon energy.[10,11]

Among chalcogenide glasses, the As–S–Se system is characterized by a large glass formation domain[12] and distinguished nonlinear properties.[4] The wide range of glass composition makes this glass an ideal candidate for tailoring important optical properties.[4] The ease of glass formation makes it desirable for low-loss optical applications. Crystalline structure in glass is one of the major reasons for optical loss.

In this context, studies of chemical and structural properties of As–S–Se glasses with different compositions are vital for understanding their optical and electronic properties. Numerous researchers have documented the molecular structure of the binary glasses in As–S,[13] As–Se,[14] and Se–S (Ref. 15) systems. To best describe the structure of the As–S glass system, the *chemically ordered network* (CON) and the *covalent random network* are compared. Many researchers[13] have concluded that statistical knowledge of chemical bonding is the key to understand the compositional dependence of the physical and optical properties of As–S glasses. Wang *et al.* adopted the CON model to represent the structure of the As–S–Se system.[16] From the CON model that favors lower-energy bonds, Wang *et al.* proposed the following three assumptions: First, only As–As, As–Se, and As–S bonds are present in arsenic-rich glass; second, As–Se, As–S, and Se–Se bonds are present in selenium-rich glass; and third, As–Se, As–S, and S–S bonds are present in sulfur-rich glasses. While CON is believed to be the model that better represents an As–S–Se three-dimensional structure, the existence of Se–Se in the sulfur-rich glass cannot be ruled out. According to Protasova *et al.*,[15] while introducing As in S–Se glass, arsenic mainly reacts with sulfur, resulting in the formation of $AsS_{3/2}$ pyramids. It is also suggested that, when the amount of S atoms is sufficient to form bonding with all the As atoms, only the $AsS_{3/2}$ pyramid is present in the glass network. The Se atoms exist in the Se–Se or Se–S chains.

In the As–S–Se ternary system, the structure and properties of $As_{40}S_{60-x}Se_x$ has been largely studied.[17,4] It possesses classic As_2Ch_3 structure, where Ch represents the chalcogen atom. Wang *et al.*[16] attempted to find the structural change with Se replacing S in the As_2Ch_3. However the glass composition ($As_{40}S_{60-x}Se_x$) was in weight percentage rather than molar substitution. It is not clear that whether

---

[a)]Author to whom correspondence should be addressed; electronic mail: sseal@pegasus.cc.ucf.edu
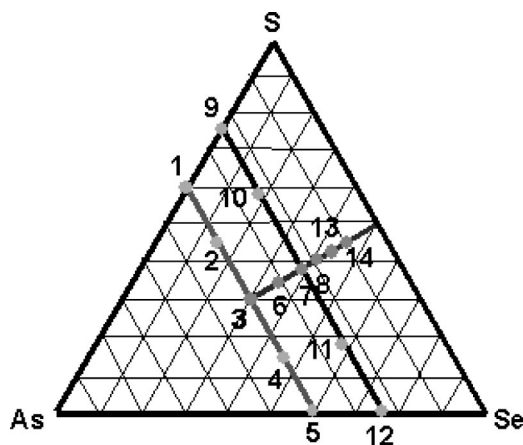
FIG. 1. The ternary composition diagram of As–S–Se system. The composition on the diagram is as follows: 1-$As_{40}S_{60}$; 2-$As_{40}S_{45}Se_{15}$; 3-$As_{40}S_{30}Se_{30}$; 4-$As_{40}S_{15}Se_{45}$; 5-$As_{40}S_{60}$; 6-$As_{32}S_{34}Se_{34}$; 7-$As_{24}S_{38}Se_{38}$; 8-$As_{18}S_{41}Se_{41}$; 9-$As_{24}S_{76}$; 10-$As_{24}S_{57}Se_{19}$; 11-$As_{24}S_{19}Se_{57}$; 12-$As_{24}Se_{76}$; 13-$As_{14}S_{43}Se_{43}$; and 14-$As_{10}S_{45}Se_{45}$.

the substitution of S by Se, or the variation of As/chalcogen ratio caused the structural change.

While the material composition plays a critical role, the fabrication process of the glass also influences the structure of these chalcogenides. Two processes, melt quenching and vapor deposition are compared in this study. The melt quenching process has been used to synthesize many amorphous chalcogenides,[18] and vapor deposition has been widely applied for thin-film fabrication.[19] The molecular configuration of the high-temperature vapor during depositing has been studied,[20] and the corresponding structure of vapor-deposited film is dominated by constituent molecular species of the vapor phase.[4] Hence, the possible composition and structure variation in the film as compared to the parent bulk glass cannot be ignored and requires further investigation.

X-ray photoelectron spectroscopy (XPS) is a useful surface analytical technique to the study of chemical state and local environment of an atom.[21–23] Important progressive alterations in chemical bonding are often realized through correlation with chemical shifts in the XPS binding energies of key elements.[21–23] For example, XPS studies have shown systematic chemical shift in oxide, nitride, and halide systems.[24,25] XPS and x-ray emission spectroscopy have been used as complementary methods to study the electronic structure of Tl_2S–Sb_2S_3 (Ref. 26) and copper chalcogenides.[27] *In situ* XPS has been shown useful in the study of the light-induced changes in As–Se glasses.[28] Other chalcogenide thin films, such as Ge–Sb–S and As–Se–Cu, have also been studied using XPS.[29,30]

In this study, XPS is applied to determine systematic chemical alternations in the chemical bonding and structure of As–S–Se glass with varying composition. The differences in the chemical structure between the bulk and the thin-film As–S–Se glasses are also examined and compared.

II. EXPERIMENT

A. Sample preparation

Materials were prepared according to an As–S–Se ternary diagram (Fig. 1), with either fixed S/Se ratio (varying As concentration), or fixed As content (varying S/Se ratio). These compositions were selected based on our understanding of As–S–Se glass structure and the unique nonlinear optical property of chalcogen rich As–S–Se composition ($As_{24}S_{38}Se_{38}$).[4]

Bulk chalcogenide glass (ChG) samples were prepared by conventional melt quenching in an evacuated silica ampoule, and the details are described elsewhere.[4] Annealed ChG samples were removed from the ampoule, cut, ground, and polished using a BUEHLER polishing machine. Bulk sample size was 10 mm in diameter, nominally 2 mm in average thickness.

Films were prepared by thermal evaporation on a slowly rotating oxidized silicon (SiO_2/Si) wafer. The evaporation rate was 1–2 nm/s and the pressure was 2×10^{-7} Torr. Small pieces of bulk glass prepared by the technique described above were used as the target material for film fabrication. Further details are described in Ref. 31.

B. XPS analysis

Surface chemistry of the bulk and the film samples was studied using a PHI 5400 ESCA at a vacuum of $\sim 10^{-9}$ Torr. A nonmonochromatic Mg–K_α x-ray source (hν = 1253.6 eV) at a power of 250 W was used for the analysis. Both survey scans and individual high-resolution scans were recorded. The survey scans were conducted from 0 to 1100 eV with a pass energy of 44.75 eV, step of 0.5 eV, and 4 sweeps. Individual high-resolution spectra (As 3d5, C 1s, S 2p3, Se 3d5, valance band) were conducted with a pass energy of 35.75 eV, step size 0.1 eV, and sweep number ranging from 20 to 50 to reach a satisfactory signal–to–noise ratio.

For insulators such as glasses, the charging effect can vary from sample to sample. As a result, the measurement of the absolute binding energy of the electrons from a specified energy level is not reliable. The C 1s line from either the adventitious hydrocarbon or intentionally added graphite powder on the surface has been widely used for charge referencing[11,32,33] For this study, the adventitious carbon was used as a reference, and the binding energy of the reference C 1s line was set as 284.6 eV.[34] For each sample, a calibration factor was calculated from the difference between the measured C 1s binding energy and the reference value 284.6 eV. The original binding energy data were corrected accordingly based on the calibration factor.

III. RESULTS AND DISCUSSION

A. XPS survey results of As–S–Se glasses

A typical survey of As–S–Se glass is shown in Fig. 2. It is to be noted that the only features above 600 eV are the Auger peaks for C and O. Both carbon and oxygen come from the surface contamination of the samples. No oxide formation is detected, as there is no observable peak separation for either As or Se individual scans. Both As and Se has many Auger peaks and energy-loss bands (see Fig. 2). The detail information about the binding energies of all those peaks can be found in Ref. 35.
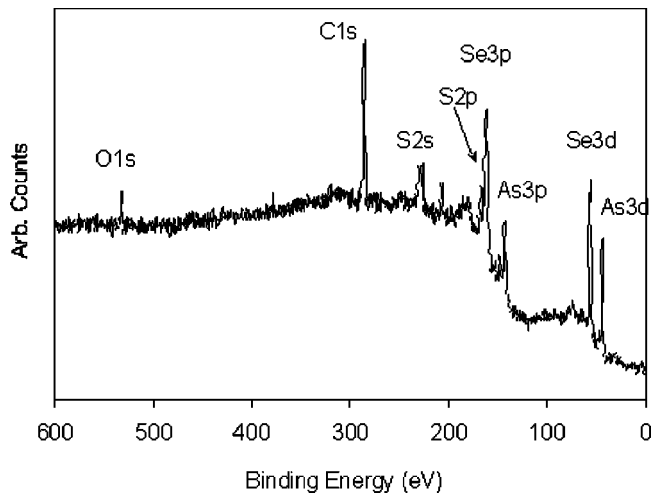
FIG. 2. A typical XPS survey spectra of As–S–Se glass.

FIG. 4. Se 3d peak in As–S–Se bulk samples with fixed As composition.

B. XPS result of As$_{24}$S$_x$Se$_{76-x}$ bulk glasses (x = 0,19,38,57,76)

XPS results of As 3d, Se 3d, and valence-band spectra of As$_{24}$S$_x$Se$_{76-x}$ bulk glasses (specimens 12, 11, 7, 10, 9) are plotted in Figs. 3, 4, and 5.

From As 3d spectra, we observe that in As$_{24}$S$_x$Se$_{76-x}$ with x increasing from 0 to 76, the binding energy of As 3d increases from 42.4 eV (As$_{24}$Se$_{76}$) to 43.0 eV (As$_{24}$S$_{76}$). Another visible feature in the spectrum is the presence of a satellite peak at 45.0 eV. This represents the Se satellite peak. The intensity of this peak increases with increasing Se concentration.

According to Georgiev *et al.*[14] the molecular structure of Se-rich As–Se glasses has been widely accepted as a random network of Se chain fragments crosslinked by pyramidal AsSe$_{3/2}$ units. The As site in S-rich As–S glasses has the similar local structure to that in crystalline As$_2$S$_3$ (orpiment), only the As–S–As linkages are replaced by As–S–S linkages at higher S concentration.[13] With the progressive replacement of Se by S, the atomic environment of As atoms changes from Se to S surrounding. The local structure of As site changes from As–Se–Se to As–S–Se and then to As–S–S. Because S is a non-metal and has a higher value of
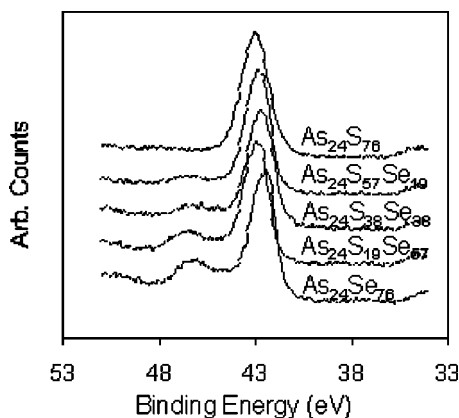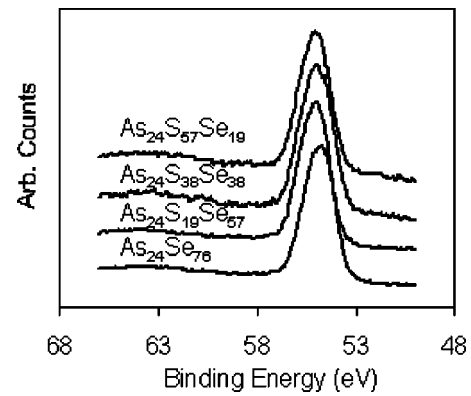
electronegativity (2.58) than that of Se (2.55),[36] the binding energy of As increases.

Figure 4 shows that the binding energy of Se 3d peak increases from 54.6 to 55.0 eV as the S/Se ratio increases. This is due to the fact that, with the substitution of Se by S, the atomic environment of Se changes from As and Se surrounding to S surrounding. The local structure of the Se site will change from As–Se–Se to S–Se–Se and then to S–Se–S. Because S has a higher electronegativity (2.58) than both Se (2.55) and As (2.18),[36] the binding energy of Se increases.

Figure 5 represents the valance-band spectra of As$_{24}$S$_x$Se$_{76-x}$ glasses. The valence band of the elemental Se sample is also detected and plotted. From Fig. 4, it was noticed that, with increasing Se, the two bands located at 2.5 and 5.5 eV become more distinct. Another feature of the valence band is that the band gap ($\Delta\varepsilon$) increases with an increasing x value, from $x=0$ (As$_{24}$Se$_{76}$) to $x=76$ (As$_{24}$S$_{76}$).

In the elemental Se valence band, the peak at 5.5 eV is associated with the bonding p band (4p), and the peak at 2.5 eV with the lone-pair orbitals.[37] These two features at the valence band of As$_{24}$S$_x$Se$_{76-x}$ glass indicate that a considerable amount of Se–Se homopolar bonds exist in a chalcogenrich As–S–Se glass system. The structure of homopolar Se–Se bonds in the As–S–Se glasses is also identified by Raman spectroscopy.[4] Meanwhile, the structural analysis

FIG. 3. As 3d peak in As–S–Se bulk samples with fixed As composition.
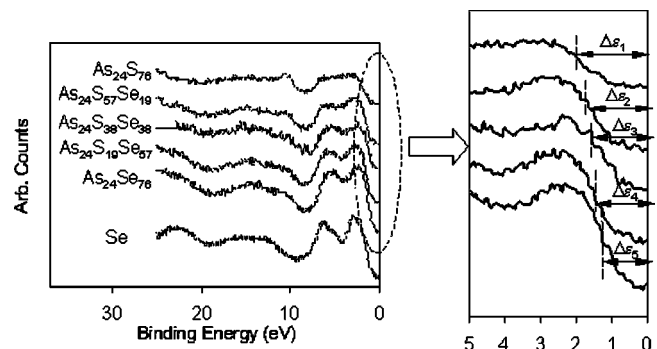
FIG. 5. Valance band in As–S–Se bulk samples with fixed as composition. In the enlarged portion, $\Delta\varepsilon_1$, $\Delta\varepsilon_2$, $\Delta\varepsilon_3$, $\Delta\varepsilon_4$, and $\Delta\varepsilon_5$ are the estimated band gap for As$_{24}$S$_{76}$, As$_{24}$S$_{57}$Se$_{19}$, As$_{24}$S$_{38}$Se$_{38}$, As$_{24}$S$_{19}$Se$_{57}$, and As$_{24}$Se$_{76}$, respectively.
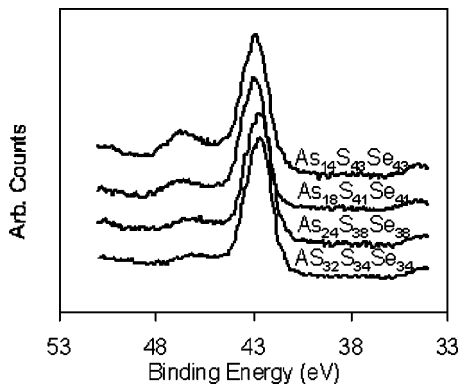
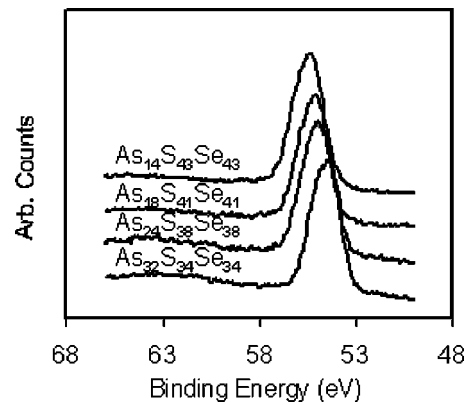FIG. 6. As $3d$ peak in As–S–Se bulk samples with fixed S/Se ratio.

FIG. 7. Se $3d$ peak in As–S–Se bulk samples with fixed S/Se ratio.

shows that the large nonlinear refractive index n_2 of the sample may be attributed to the excess of Se–Se or Se–S covalent bonds. This supports the premise that increasing covalency between polarizable atoms increases n_2.[4,38] According to the valence-band spectra of $As_{24}S_xSe_{76-x}$, introducing Se into chalcogen-rich As–S–Se glasses, the amount of Se–Se homopolar bands increases, so does the nonlinear property n_2.

Another important observation we gain from the valance-band data is the band-gap information. The band gap of insulator between the valence band and the empty conduction band can be calculated from the high-resolution XPS result of the valence band after Fermi-level correction.[39,40] Here, we estimate the band gap at the valence-band leading edge.[24] We can see an appreciable decrease in the band gap with increasing Se, from about 2.0 ($As_{24}S_{76}$) to 1.4 eV ($As_{24}S_{76}$). The corresponding optical band gap, or to be exact, the optical absorption (OA) maximum, instead of the optical absorption edge,[40] is shifted from 620 to 830 nm (near IR range).

The OA redshift effect caused by the substitution of S by Se has an important impact on the IR application of the glasses. Similar results have been observed in the linear optical absorption spectra of the $As_{40}S_{60-x}Se_x$ system.[4] It is also important to consider band-gap information for higher-power application, where a glass's two-photon absorption (2PA) becomes significant. For use at the telecommunication wavelength of 1.55 μm, the two-photon energy (2hν) is about 1.6 eV. Hence, glasses with a band gap near or below this level, may have appreciable 2PA nonlinear absorption that could compromise the materials use in high power applications.[41] Based on this observation, excessive Se composition should be avoided when we use $As_{24}S_xSe_{76-x}$ glass for high-energy applications. These glasses may have band gaps lower than the 2PA energy.

C. XPS result of $As_{100-2x}S_xSe_x$ bulk glasses ($x=34,38,41,43$)

XPS results of As $3d$, Se $3d$, and valence bands of the $As_{100-2x}S_xSe_x$ bulk glasses (Specimens 6, 7, 8, and 13) are plotted in Figs. 6, 7 and 8.

In Fig. 6, for $As_{100-2x}S_xSe_x$, where x increases from 34 to 43, with fixed S/Se$=1$ and a decrease in As content, the

binding energy of As $3d$ increases from 42.6 to 43.0 eV. The Se satellite is also present, and its intensity increases as Se to As ratio increases.

The molecular structure of chalcogen-rich As chalcogenide glass is made of chalcogen chain fragments cross linked by $AsCh_{3/2}$ units.[13,14] From $As_{32}S_{34}Se_{34}$ to $As_{14}S_{43}Se_{43}$, (S $+$ Se)/As ratio increasing from 2.1 to 6.1, the number of As-containing pyramid units is expected to decrease and chalcogen–chalcogen chain length to increase. It has been observed by Raman spectroscopy that, in chalcogen-rich glasses containing equal amounts of S and Se, S primarily forms As–S bonds and Se forms homopolar Se–Se, or heterpolar S–Se bonds.[4] As the arsenic content is reduced and the chalcogen molar ratio Se/S remains equal to one, the atomic environment of As atom changes from S and Se surrounding to S surrounding. The local environment of the As site changes from Se–As–S to S–As–S. Because S has a higher electronegativity than Se, the binding energy of As $3d$ increases.

Figure 7 shows that with increasing x, the Se $3d$ binding energy of $As_{100-2x}S_xSe_x$ increases from 54.5 eV ($As_{32}S_{34}Se_{34}$) to 55.5 eV ($As_{14}S_{43}Se_{43}$). With decreasing As content, the atomic environment of Se changes from As and S surrounding to S and Se surrounding. Hence, the local structure of Se changes from As–Se–S to S–Se–Se. That causes the binding energy of Se $3d$ to increase.
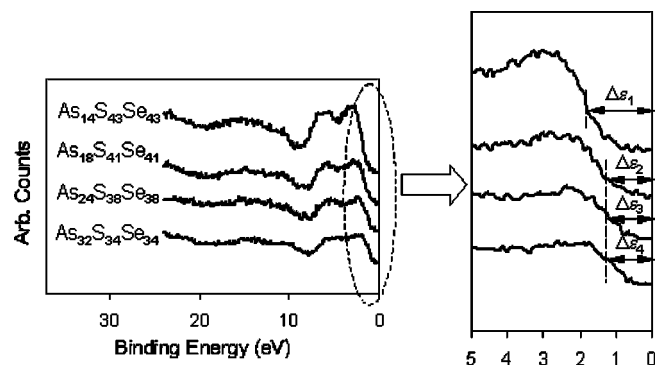

FIG. 8. Valance band in As–S–Se bulk samples with fixed Se/S ratio. In the enlarged portion, $\Delta\varepsilon_1$, $\Delta\varepsilon_2$, $\Delta\varepsilon_3$, and $\Delta\varepsilon_4$ are the estimated band gap for $As_{14}S_{43}Se_{43}$, $As_{18}S_{41}Se_{41}$, $As_{24}S_{38}Se_{38}$, and $As_{32}S_{34}Se_{34}$, respectively.

In Fig. 8, with decreased As and fixed S/Se$=1$, the valence-band spectra shows that the two bands located at 2.5 and 5.5 eV become more distinct, a typical characteristic of the elemental Se valence band. This confirms that there will be more Se in the Se–Se and Se–S chains with decreasing As, as S is mainly participating in the AsS$_{3/2}$ pyramidal units.

Unlike in As$_{24}$S$_x$Se$_{76-x}$ glasses, there is no clear pattern of the band-gap changes in the As$_{100-2x}$S$_x$Se$_x$ system. While the band-gap energies of As$_{18}$S$_{41}$Se$_{41}$, As$_{24}$S$_{38}$Se$_{38}$, and As$_{32}$S$_{34}$Se$_{34}$ are almost the same, As$_{14}$S$_{43}$Se$_{43}$ seems to have a higher value. Prior optical absorption measurement[4] also found that the decrease in the molar ratio As/(S+Se) has little effect on the linear absorption, and the optical band edge remained in the same wavelength range for As$_{24}$S$_{38}$Se$_{38}$, As$_{32}$S$_{34}$Se$_{34}$, and As$_{40}$S$_{30}$Se$_{30}$.

In the As–S binary system, a decrease in As/S ratio results in a systematic increase in the band gap.[38] From As$_{40}$S$_{30}$Se$_{30}$ to As$_{24}$S$_{38}$Se$_{38}$, the As/Ch ratio decreases, however the band gap shows little change. This result can be explained by two factors that compensate each other. First, from As$_{40}$S$_{30}$Se$_{30}$ to As$_{24}$S$_{38}$Se$_{38}$, the decrease in the As/S ratio causes an increase in the band gap. Second, the increase in Se concentration, meaning more Se–Se or Se–S bonds,[4] causing a decrease in band gap.

The reason for As$_{14}$S$_{43}$Se$_{43}$ having a higher-band gap than the reference value[41] is not clear. One possible reason is that the XPS data collection was done on an old sample for this composition. It took longer (more than 30 min) to sputter clean the sample. All the other fresh samples required 5–10 min to sputter away most of the surface contamination and achieve good signal–to–noise ratio. The long sputtering time may have affected the sample surface chemistry to induce change in the band gap. It was found that, in the Se sample, Ar$^+$ bombardment produced reversible changes of the structure in the XPS valence band which relaxes during a time interval of days. The $4p$ bonding and the lone-pair orbits tend to merge to one peak at a binding energy close to the lone-pair orbit.[42] While the lone-pair orbit shifts to a higher-binding energy, the band gap increases. The high-Se composition may cause similar change in As$_{14}$S$_{43}$Se$_{43}$, under ion bombardment, even though the merging of the two peaks is not completed. This could be a reason for the higher-band gap in As$_{14}$S$_{43}$Se$_{43}$.

Another possible reason might be due to the fact that As and Se–S bands have different conductivity. As a result, the As$_{1-x}$(SSe)$_x$ compound will show a change in the band gap with changing x value, especially at the end compositions (As and S$_{50}$Se$_{50}$). When the composition is close to S$_{50}$Se$_{50}$, an increase of band gap will occur. This may also explain the higher-band gap in As$_{14}$S$_{43}$Se$_{43}$.

D. Comparing film and bulk As$_{100-2x}$S$_x$Se$_x$ samples ($x=34,38,41,43$)

Thin-film devices based on chalcogenide glasses are attractive for integrated optics applications due to their good infrared transmission and high-nonlinear Kerr effects.[43] To optimize film properties and device performance, we use XPS to identify the chemical and structural origin of the
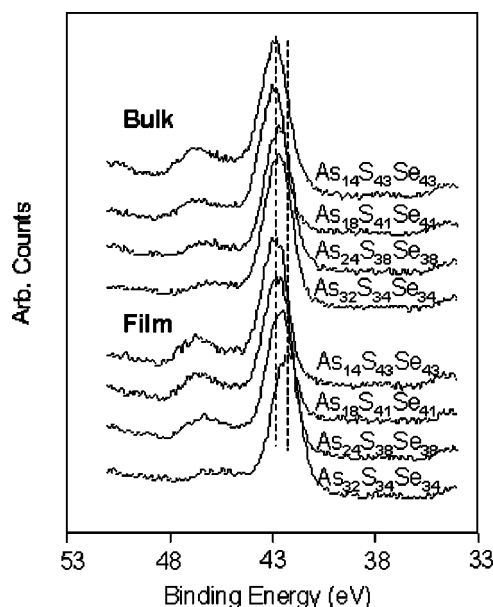

FIG. 9. Comparing As $3d$ peaks between bulk and film samples with fixed S/Se ratio.

thin-film optical properties, and compare it to bulk samples, where the processing conditions are vastly different.

A detailed comparison was made between the bulk and the film samples with fixed S/Se ratios in Figs. 9, 10 and 11. Here, similar trends are observed in film as in bulk, but two distinct differences are observed. First, the two peaks at 2.5 and 5.5 eV in the valance band are more distinct and sharper in film samples. Second, both the binding energies for As $3d$ and Se $3d$ are slightly lower in the films than in the bulk samples.

The structural difference between bulk and film chalcogenide glasses has been well studied in the As–S and As–Se
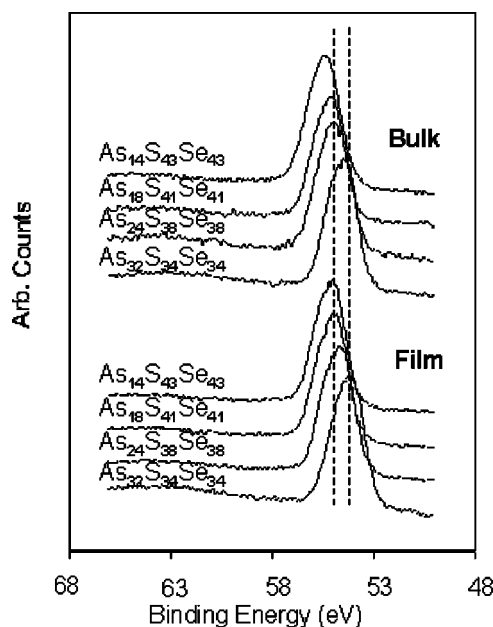

FIG. 10. Comparing Se $3d$ peaks between bulk and film samples with fixed S/Se ratio.

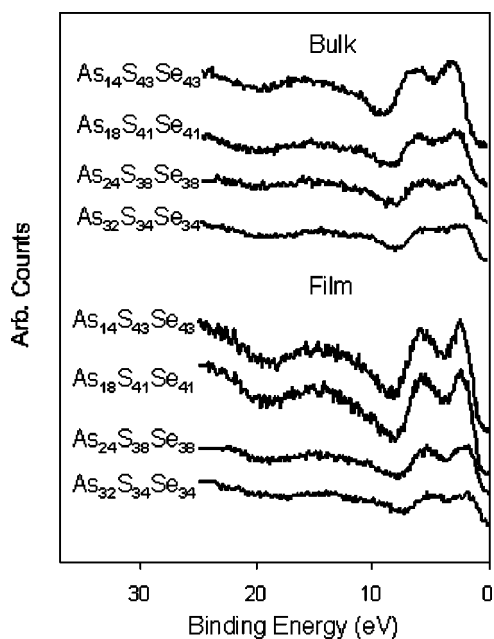J. Appl. Phys., Vol. 92, No. 12, 15 December 2002

Li *et al.* 7107

FIG. 11. Comparing valance bands between bulk and film samples with fixed S/Se ratio.

binary systems. The x-ray diffraction study shows that the structure of the freshly deposited As_xSe_{1-x} film differs very significantly from that of the bulk glass.[44] In As_2Se_3 film, optical measurement observed two absorption bands which were interpreted in terms of defect of homopolar bonds.[45] In arsenic sulfide film, there is evidence of more As–As bonds; and the films are As rich.[46] Recent research confirmed that As–S film contains at least 32% of As–As bonds in the total arsenic bonds, and the amount of As–As bonds decreases after annealing and illumination.[47]

The structural difference between bulk and film As–S–Se ternary glass is rarely studied. The Raman study[17] on $As_{40}S_{40}Se_{20}$ suggested that mixed $AsS(Se)_{3/2}$ pyramidal structural units present in the structure of as-evaporated films; the film may contain a significant number of defects such as $As_4S(Se)_4$, $S(Se)$, and As_4 molecular fragments; and there is evidence for As–As bonds.

It is evident from our studies, $As_4S(Se)_4$ is present in chalcogen-rich As–S–Se glassy films, as As_4Ch_4 is the dominant species in the vapor phase.[47] Earlier Raman study[43] on chalcogenide film also suggested a similar existence of as-deposited molecular As_4S_4 units. Thus, arsenic atoms in films may possess a lower-coordination number, resulting in a lower As $3d$ binding energy.

Another effect of the structural difference, is that the network of the glass film is weaker, and more molecular fragments such as $S(Se)$ and As_4 exist.[17] This means there are more homopolar bonds (As–As, S–S, and Se–Se bonds). That also results in a lower Se $3d$ binding energy.

Film valence-band results showed that the Se-elemental band structures are more distinct and sharper. These findings confirm that there are more Se–Se bands in the films than in the bulk samples (i.e., higher peaks in valence-band features). It also supports the existence of Se molecular fragment (i.e., sharper peaks in valence band). It was found that

the excess of Se–Se covalent bonds are responsible for the higher nonlinearity in As–S–Se glasses.[4] As the structure and the composition of evaporated chalcogenide films depends strongly on the preparation conditions of their bulk parent glass and the evaporation conditions,[48] it is possible to improve the nonlinearity of the As–S–Se films through controlling the conditions of the film formation.

IV. CONCLUSIONS

In summary, we studied the compositional structural changes in a chalcogen-rich As–S–Se system using As $3d$, Se $3d$, and valence-band XPS results from $As_{24}S_xSe_{76-x}$ and $As_{100-x}S_xSe_x$ glasses. The following are the important conclusions of this study:

(1) In $As_{24}S_xSe_{76-x}$, with fixed As=24% and Se replaced by S, increasing x results in an increase in the As $3d$ and Se $3d$ binding energies. At higher Se concentration, a considerable amount of Se–Se homopolar bonds exist in the glass. This can result in an appreciable redshift in the optical band gap with increasing Se content.

(2) In $As_{100-2x}S_xSe_x$, with fixed S/Se=1, decreasing As in the glass, similar increase in the XPS binding energies of As $3d$ and Se $3d$ has been observed. At lower As concentration, there are more Se–Se bonds in the glass structure. There is no considerable change in the optical band gap caused by changing the As content in $As_{100-2x}S_xSe_x$, from $x=34$ to $x=41$.

(3) The results from the As–S–Se films are similar to that of the bulk glasses, but there are two major differences. First, in the films, the binding energies of both As $3d$ and Se $3d$ are slightly lower than those in the bulk samples. Second, the features of Se–Se homopolar bonds are more distinguished and sharp in the films as detected from XPS valence bands. More importantly, this feature shows the evidence of the existence of molecular fragments of $As_4S(Se)_4$, S–S, and Se–Se in the film structure.

[1] R. Frerichs, Phys. Rev. **78**, 643 (1950).

[2] R. Frerichs, J. Opt. Soc. Am. **43**, 1153 (1953).

[3] A. R. Hilton, J. Non-Cryst. Solids **2**, 28 (1970).

[4] T. Cardinal, K. A. Richardson, H. Shim, A. Schulte, R. Beatty, K. Le Foulgoc, C. Meneghini, J. F. Viens, and A. Villeneuve, J. Non-Cryst. Solids **256&257**, 353 (1999).

[5] D. W. Hall, M. A. Newhouse, N. F. Borrelli, W. H. Dumbaugh, and D. L. Weidman, Appl. Phys. Lett. **54**, 1293 (1989).

[6] O. M. Efimov, L. B. Glebov, K. A. Richardson, E. Van Stryland, T. Cardinal, S. H. Park, M. Couzi, and J. L. Bruneel, Opt. Mater. **17**, 379 (2001).

[7] A. V. Stronski, M. Vlcek, A. Sklenar, P. E. Shepeljavi, S. A. Kostyukevich, and T. Wagner, J. Non-Cryst. Solids **266−269**, 973 (2000).

[8] M. Asobe, K. Suzuki, T. Kanamori, and K. Kubodera, Appl. Phys. Lett. **60**, 1153 (1992).

[9] A. Saliminia, A. Villeneuve, T. V. Galstyan, S. LaRochelle, and K. Richardson, J. Lightwave Technol. **17**, 837 (1999).

[10] W. E. Morgan and J. R. Van Wazer, J. Phys. Chem. **77**, 964 (1973).

[11] J. F. Moulder, W. F. Sticker, P. E. Sobol, and K. D. Bomben, *Handbook of X-ray Photoelectron Spectroscopy* (Perkin-Elmer, Eden Prairie, MN, 1992).

[12] M. A. Popescu, *Non-Crystalline Chalcogenides* (Kluwer Academic, Boston, 2000).

[13] C. Y. Yang, A. A. Paesler, and D. E. Sayers, Phys. Rev. B **39**, 10 342 (1989), and references within.

[14] D. G. Georgiev, P. Boolahand, and M. Micoulaut, Phys. Rev. B **62**, R9228 (2000).

[15] L. G. Protasova, P. I. Buler, and S. A. Subbotina, Inorg. Mater. (Transl. of Neorg. Mater.) **25**, 659 (1989).

[16] J.-L. Wang, J.-C. Tsai, C.-T. Liu, P. Nachimuthu, L.-Y. Jang, R.-G. Liu, and J.-M. Chen, J. Appl. Phys. **88**, 2533 (2000).

[17] M. Vlcek, A. V. Stronki, A. Sklenar, T. Wagner, and S. O. Kasap, J. Non-Cryst. Solids **266−269**, 964 (2000).

[18] E. Hartouni, F. Hulderman, and T. Guiton, Proc. SPIE **505**, 131 (1984).

[19] S. A. Keneman, Thin Solid Films **21**, 281 (1974).

[20] A. C. Wright, R. N. Sinclair, and A. J. Leadbetter, J. Non-Cryst. Solids **71**, 295 (1985).

[21] P. I. K. Onorato, M. N. Alexander, C. W. Struck, G. W. Tasker, and D. R. Uhlmann, J. Am. Ceram. Soc. Bull. **68**, C148 (1985).

[22] J. Heo, J. S. Sanghera, and J. D. Mackenzie, J. Non-Cryst. Solids **101**, 23 (1988).

[23] R. M. Almeida, H. Nasu, J. Hoe, and J. D. Mackenzie, J. Mater. Sci. Lett. **6**, 701 (1987).

[24] D. Briggs and M. P. Seah, *Practical Surface Analysis*, 2nd ed. Auger and X-ray Photoelectron Spectroscopy (Wiley, Chichester, England, 1990), Vol. 1.

[25] S. J. Kerber, J. J. Bruckner, K. Wozniak, S. Seal, S. Hardcastle, and T. L. Barr, J. Vac. Sci. Technol. A **14**, 1314 (1996).

[26] A. Gheorghiu, I. Lampre, S. Dupont, C. Senemaud, M. A. El Idrissi Raghni, P. E. Lippens, and J. Olivier-Fourcade, J. Alloys Compd. **228**, 143 (1995).

[27] E. P. Domashevskaya, V. V. Gorbachev, V. A. Terekhov, V. M. Kashkarov, E. V. Panfilova, and A. V. Shchukarev, J. Electron Spectrosc. Relat. Phenom. **114−116**, 901 (2001).

[28] H. Jain, S. Krishnaswami, A. C. Miller, P. Krecmer, S. R. Elliott, and M. Vlcek, J. Non-Cryst. Solids **274**, 115 (2000).

[29] L. Jiang, A. G. Fitzgerald, M. J. Rose, K. Christova, and V. Pamukchieva, J. Non-Cryst. Solids **297**, 13 (2002).

[30] M. Bruns, H. Klewe-Nebenius, G. Pfennig, E. Bychkov, and H. J. Ache, Surf. Coat. Technol. **97**, 707 (1997).

[31] J. Fick, E. J. Knystautas, A. Villeneuve, F. Schiettekatte, S. Roorda, and K. A. Richardson, J. Non-Cryst. Solids **272**, 200 (2000).

[32] W. J. Stec, W. E. Morgan, R. G. Albridge, and J. R. Van Wazer, Inorg. Chem. **11**, 219 (1972).

[33] W. E. Morgan and J. R. Van Wazer, J. Phys. Chem. **77**, 964 (1973).

[34] T. L. Barr and S. Seal, J. Vac. Sci. Technol. A **13**, 1239 (1995).

[35] B. Vincent Crist, *Handbook of Monochromatic XPS Spectra—The Elements and Native Oxides* (Wiley, New York, 2000), Vol. 1.

[36] *CRC Handbook of Chemistry and Physics*, edited by David R. Lide, 78th ed. (CRC, Press LLC, Boca Raton, FL, 1997).

[37] N. J. Shevchik, M. Cardona, and J. Tejeda, Phys. Rev. B **8**, 2833 (1973).

[38] E. Hajto, P. J. S. Ewen, A. E. Owen, J. Non-Cryst. Solids **164−166**, 901 (1993).

[39] G. Martin, S. Strite, A. Botchkarav, A. Agarwal, A. Rockett, H. Morkoc, W. R. Lambrecht, and B. Segall, Appl. Phys. Lett. **65**, 610 (1994).

[40] L. S. Lian, M. K. Fung, C. S. Lee, S. T. Lee, M. Inbasekaran, E. P. Woo, and W. W. Wu, Appl. Phys. Lett. **76**, 3582 (2000).

[41] A. Schulte and K. Richardson, (unpublished).

[42] B. R. Orton and J. C. Riviere, J. Non-Cryst. Solids **37**, 401 (1980).

[43] A. Schulte, C. Rivero, K. Richardson, K. Turcotte, V. Hamel, A. Villeneuve, T. Galstian, and R. Vallee, Opt. Commun. **198**, 125 (2001).

[44] A. J. Leadbetter, A. J. Apling, and M. F. Daniel, J. Non-Cryst. Solids **21**, 47 (1976).

[45] M. M. El-Ocker, F. Sharaf, and M. K. El-Mously, J. Mater. Sci. **27**, 1157 (1992).

[46] A. J. Apling, A. J. Leadbetter, and A. C. Wright, J. Non-Cryst. Solids **23**, 369 (1977).

[47] F. Kosek, Z. Cimpl, J. Tulka, and J. Chlebny, J. Non-Cryst. Solids **90**, 401 (1987).

[48] T. Bando, D. P. Gosain, S. Okano, and M. Suzuki, Thin Solid Films **195**, 237 (1991).